HHS Public Access

Author manuscript

Oncogene. Author manuscript; available in PMC 2013 August 28.

Published in final edited form as:

Oncogene. 2013 February 28; 32(9): 1193–1201. doi:10.1038/onc.2012.120.

Mitochondrial genome instability resulting from SUV3 haploinsufficiency leads to tumorigenesis and shortened lifespan

Phang-Lang Chen[1,*], **Chi-Fen Chen**[1], **Yumay Chen**[2], **Xuning Emily Guo**[1], **Chun-Kai Huang**[3], **Jin-Yuh Shew**[3], **Robert L. Reddick**[4], **Douglas C. Wallace**[5], and **Wen-Hwa Lee**[1,3,*]

[1]Department of Biological Chemistry, School of Medicine, University of California, Irvine, CA.

[2]Department of Medicine, School of Medicine, University of California, Irvine, CA.

[3]Genomics Research Center, Academia Sinica, Taipei, Taiwan.

[4]Department of Pathology, University of Texas Health Science Center at San Antonio, TX.

[5]Department of Biological Chemistry and Center for Molecular & Mitochondrial Medicine and Genetics, School of Medicine, University of California, Irvine, CA.

Abstract

Mitochondrial dysfunction has been a hallmark of cancer. However, whether it plays a causive role awaits to be elucidated. Here, using an animal model derived from inactivation of SUV3, a mitochondrial helicase, we demonstrated that *mSuv3*+/− mice harbored increased mtDNA mutations and decreased mtDNA copy numbers, leading to tumor development in various sites and shortened lifespan. These phenotypes were transmitted maternally, indicating the etiological role of the mitochondria. Importantly, reduced SUV3 expression was observed in human breast tumor specimens compared to corresponding normal tissues in two independent cohorts. These results demonstrated for the first time that maintaining mtDNA integrity by SUV3 helicase is critical for cancer suppression.

Keywords

mitochondrial dysfunction; Suv3; animal model; tumorigenesis

[*]To whom correspondence should be addressed: Wen-Hwa Lee: 124 Sprague Hall, Irvine, CA 92697-4037. Tel: 949-824-4492 whlee@uci.edu, Phang-Lang Chen: Med Sci 1, Room D252, Irvine, CA 92697-4037. Tel: 949-824-4008, plchen@uci.edu.

Contributions

P.L.C. and W.H.L. conceptualized experiments, prepared figures and drafted the manuscript. C.F.C. performed majority of the experiments. Y.C. performed the time pregnancy analysis. X.E.G. performed cell experiments. J.Y.S. and C.K.H analyzed of the SUV3 expression level in human tumor specimens, R.L.R. analyzed histology experiments. D.C.W. provided scientific advice and critical comments on manuscript.

Competing financial interests

The authors declare no competing financial interests.

Introduction

The mitochondria generate most of the cellular ATP and reactive oxygen species (ROS), regulate cellular calcium levels, and initiate cell death through the activation of the mitochondrial permeability transition pore (1, 2). Each mammalian cell contains hundreds of mitochondria and each mitochondrion contains multiple copies of circular mitochondrial DNA (mtDNA) molecules. The mtDNA encodes 13 polypeptides central to the mitochondrial energy production system, oxidative phosphorylation (OXPHOS), as well as the rRNAs and tRNAs necessary for mitochondrial protein synthesis. The mtDNA is replicated from two origins, one for the G-rich heavy (H) strand located in the control region and the other for the C-rich light stand located 2/3 of the way around the mtDNA (3). Cells have developed extensive systems for maintaining mitochondrial integrity and disturbance of mitochondrial homeostasis can lead to multiple diseases (2). In general, the mtDNA has a higher mutation rate than nuclear DNA (nDNA) genes. The accumulation of mtDNA mutations has not only been linked to ageing (2, 4, 5, 6), but also to cancer progression (7, 8). However, the causative roles of mitochondrial genome integrity in ageing and cancer remain to be substantiated.

SUV3 is a nuclear encoded ATP-dependent DNA/RNA helicase that primarily localizes to the mitochondrion. In *Saccharomyces cerevisiae*, Suv3 is a key component of the mitochondrial RNA degradosome besides the Dss1 exoribonuclease (9, 10, 11). Deficiency of SUV3 is associated with group I intron accumulation (10) and changes in the stability and processing of several mitochondrial RNAs (11). Yeast cells carrying null or mutant *Suv3* genes gradually lose their capacity to grow on non-fermentable carbon sources and acquire a petite phenotype (12, 13). In human cells, depletion of SUV3 by siRNA leads to pleiotropic effects including decreased mtDNA copy number, a shift in mitochondrial morphology from tubular to granular, and eventual senescence or cell death (14). While the yeast *Suv3* and mammalian *SUV3* genes sharhe high sequence homology, salient differences between the two species such as the absence of Dss1 in human mitochondria and the lack of introns in mammalian mtDNA raises the question of whether the yeast and mammalian SUV3 serve analogous mitochondrial functions.

To clarify the function of mammalian SUV3, we generated a mouse *Suv3* (*mSuv3*) knockout mouse. The homozygous *mSuv3* knockout mice were embryonic lethal, suggesting an essential role of *mSuv3* in embyronic development. Heterozygous (*mSuv3*+/−) animals, on the other side, had a shortened lifespan, reduced fecundity, and increased tumor incidence. More intriguingly, such effects were maternally transmitted, as only the mother but not the father, harboring the mutated *mSuv3* gene, could transmit the defects to subsequent generations regardless the progenies' nDNA genotype. The progenies of *mSuv3*+/− females showed elevated mtDNA mutation loads and reduced mtDNA copy numbers. These data suggest that SUV3 is a tumor suppressor gene that inactivation of one allele leads to destablization of mtDNA integrity, causing the observed detrimental effects in mice. Based on the fact that *mSuv3*+/− mice showed an increased tumor incidence, we quantitated the SUV3 mRNA level in two independent cohorts of human breast cancer specimens. We found that SUV3 mRNA expression was significantly reduced in tumor samples compared to adjacent normal tissue a panel of breast cancer specimens. Taken together, our data

indicated that reduction of SUV3 expression level, either by genetic ablation of one allele of *Suv3* in mice or other unknown mechanisms in human, could lead to destablization of mtDNA and promotes tumorigenesis, further supporting the notion that SUV3 is a potential human tumor suppressor that functions in a haploinsufficient manner.

Results

Targeted disruption of the *mSuv3* locus leads to embryonic lethality

To test if deficiency in mammalian SUV3 would lead to detrimental effect in animal as a whole as it does in yeast, we inactivated the *mSuv3* gene in embryonic stem (ES) cells to generate a knockout mouse model for SUV3. The *mSuv3* gene was obtained by screening a 129/Sv-derived genomic library using the human *SUV3* cDNA as a probe. The targeting vector, *mSuv3*-KO, was constructed by inserting an anti-parallel *pgkneopA* cassette into the *mSuv3* location corresponding to codon 684 of the human SUV3, which rendered the SUV3 mRNA unstable and blocked SUV3 expression. The successfully targeted ES cells were used to generate chimeric mice, which ultimately resulted in germ line transmission of the knockout gene (Fig. 1A). An approximate 50% reduction in SUV3 protein level was observed in *mSuv*3 heterozygous (*mSuv3*+/−) mouse embryonic fibroblasts (MEF) when compared to the wild type MEF (Fig. 1B). There was no detectable truncated SUV3 protein in heterozygous MEF, further indicating that the knockout allele is a null depletion of SUV3.

The *mSuv3*+/− mice were interbred and the genotypes of the offspring were determined at 10 days of age by PCR analysis of toe DNA. Out of the 74 animals screened, 52 were heterozygous (*mSuv3*+/−) and 22 were wild type (*mSuv3*+/+) with no homozygous mutant (*mSuv3*−/−), suggesting that the *mSuv3*−/− embryos are non-viable, which is consistent with previously described (15). To pinpoint the time of death, pregnant females of E5.0 to E11.5 from *mSuv3*+/− intercrosses were sacrificed and the fetuses were subjected to genotyping. At both E9.5 and E11.5, no *mSuv3*−/− embryos was found; instead, many resorbed embryos were present. Hence, the *mSuv3* −/− embryos died by E9.5 (Fig. 1C).

To further characterize the developmental defects, decidual swellings from *mSuv3*+/− intercrossed females were obtained between embryonic E5.0 to E8.5, and examined histologically following staining with hematoxylin/eosin. As shown in Fig. 1D, both *mSuv3*+/+ and *mSuv3*+/− embryos exhibited normal growth, depicted by the elongation of the egg cylinder and formation of embryonic and extra-embryonic ectoderm, as well as distinct proamniotic cavities. By contrast, *mSuv3*−/− embryos presented abnormalities following implantation (E5.0 to E5.5), as they were smaller and failed to form the typical egg cylinders. By the time when *mSuv3*+/+ embryos underwent gastrulation (E7.5 to E8.0), the growth of *mSuv3*−/− embryos were remarkably delayed. By E8.5, the *mSuv3*−/− embryos started to degenerate and were resorbed, consistent with aforementioned genotyping results (Fig. 1C).

Shortened lifespan of *mSuv3* heterozygotes at different intercross generations

To monitor the effect of *mSuv3* mutation over generations, we carried out a systematic studies on intercrossed mice. The first generation (F1) of heterozygous *mSuv3*+/− mice obtained by crossing the chimeric founder male with C57/BL6 female had normal lifespan comparable to the *mSuv3*+/+ wild type mice (Fig. 2A). However, the second generation (F2) of *mSuv3*+/− heterozygotes derived from intercrossing F1 heterozygotes had significantly shortened lifespan, which was aggravated in subsequent intercrosses of *mSuv3*+/− mice for the third and forth generations (F3 and F4, respectively). In addition, some of the intercross heterozygous (*mSuv3*+/−) mice showed signs of premature ageing including kyphosis (data not shown). These data suggested that inactivating one allele of *mSuv3* leads to reduced longevity over generations.

SUV3 acts as a tumor suppressor with haploinsufficiency

Through pathological examinations, we found high incidence of solid tumors in *mSuv3*+/− mice. On autopsy, 90% of the *mSuv3*+/− intercross mice exhibited a broad spectrum of tumor types, including lymphoma and carcinoma (Fig. 2B & 2C). It was noted that about two thirds of the *mSuv3*+/− mice succumbed to lymphoma. The *mSuv3*+/− tumor incidence was substantially higher than the 30% incidence seen in the *mSuv3*+/+ mice from similar genetic crosses. To determine if the tumors in *mSuv3*+/− mice acquired a second mutation in the wild type *mSuv3* allele, we isolated tumor cells by micro-dissections (Fig. 2D) and analyzed the wildtype *mSuv3* locus by PCR. As shown in Fig. 2E, all of tumor samples retained the wild type *mSuv3* allele. This was further confirmed by immunostaining with anti-SUV3 antibodies as the majority of tumor samples were SUV3 positive (Fig. 2F). These data combined indicated that loss of 50% of SUV3 protein, by genetic ablation of one *mSuv3* allele, is sufficient to predispose the mice for tumorigenesis.

Mitochondrial function is a dominant determinant for *mSuv3* inheritance

In the course of analyzing the third generation intercrossed *mSuv3*+/− mice, we found that even the *mSuv3*+/+, the mice carrying two wild type *mSuv3* alleles, showed shortened lifespan and were prone to tumors at a comparable level to that of their *mSuv3*+/− littermates (Fig. 3A and Fig. 2B). This observation suggested that the reduced lifespan and increased tumor incidence were not simple consequences of the nuclear DNA genotype. Since SUV3 has been shown to be important in maintaining mitochondrial homeostasis (14), we investigated if a maternal factor might be contributing to the progressively declined lifespan and increased tumor incidence in *mSuv3*+/+ mice of F3. Accordingly, we crossed F3 *mSuv3*+/− males with C57/BL6 wildtype females. As shown in Fig. 3B, the average lifespan of the heterozygous offspring with wild type mitochondria inherited from their mothers was 782 days, which was comparable to that of the first generation cohort (801 days). In contrast, when F3 *mSuv3*+/− females were crossed with C57/BL6 males, the average lifespan of the their heterozygotes offsprings carrying mitochondria from their *mSuv3*+/− mothers was 559 days, simlar to the lifespan of the F3 mice (Fig. 3B). Moreover, the *mSuv3*+/+ wild type offsprings generated from crossing F3 *mSuv3*+/− females with C57/BL6 males also had reduced average lifespan of 631 days (Fig. 3C), which was significantly shorter than that of the heterozygous mice (*mSuv3*+/−) with mitochondria

derived from wild type female (782 days), but not statistically different from the average lifespan (560 days) of offspring from *mSuv3*+/− females (P=0.37) (Fig. 3B). Autopsies performed on *mSuv3*+/+ offsprings derived from *mSuv3*+/− female by C57/BL6 male crosses revealed presence of tumor nodules, predominately lymphoma and pituitary adenoma, with nearly complete penetrance (Fig. 3C). Apparently, the status of mitochondria on the maternal side determines the outcome of the lifespan and tumor incidence in their offsprings, rather than their own nDNA genotype in terms of *mSuv3*.

Similarly, the reproductive performance of the *mSuv3*+/− strain also depends on the status of mitochondria function. The litter size and number of viable pups of the F1 and F2 *mSuv3*+/− intercrossed mice were comparable to that of the wild type mice (6–8 pups) (Fig. 4A & B). However, the reproductive output of such female declined in F3 (Fig. 4C). Severe reduction in reproductive performance was also found in the *mSuv3*+/+ F4 female (Fig. 4D). Besides, these *mSuv3*+/+*; mt-msuv3*+/− pups that did survive were found to be sterile at 3–5 months of age, further suggesting the dominance of mitochondrial status over nuclear genotype. In the subsequent part of this communication, we designated the mitochondria derived from an *mSuv3*+/− female as (*mt-msuv3*+/−) and that from an *mSuv3*+/+ female as (*mt-msuv3*+/+).

Increased mutation load and reduced mtDNA copy number correlate with high tumor incidence and shortened lifespan

To test whether mtDNA serves as the key factor that determines the maternally transmitted defects, we generated four genotype cohorts of mice by crossing *mSuv3*+/− male or female mice with C57/BL6 mice: Cohort A: *mSuv3*+/+*; mt-msuv3*+/+; Cohort B: *mSuv3*+/−*; mt-msuv3*+/+; Cohort C: *mSuv3*+/+*; mt-msuv3*+/−; and Cohort D: *mSuv3*+/−*; mt-msuv3*+/− (Fig. 5A). Then, mtDNA mutation load and mtDNA copy number of these four cohorts of mice were analyzed. A DNA region surrounding the L-strand replication origin (nt 4418–6409) was sequenced to assess mtDNA mutation load. As shown in Fig 5A, the levels of new mtDNA mutations were increased about 3 folds in Cohorts B, C, and D compared to age-matched Cohort A or C57/BL6 mice. This data suggested that the deficiency of SUV3 increases mtDNA mutations load. Once the mtDNA mutations have been predisposed, they are stable and transmitted through the female germline, which may not be affected by nuclear genotype.

To further characterize the effects of the *mSuv3*+/− genotype on mtDNA metabolism, we analyzed the mtDNA to nDNA copy number ratio on the spleens of 15-month-old mice, quantified by real time PCR using mtDNA 12S rRNA and nDNA 18S rRNA primers (Fig. 5B). The mtDNA copy number was markedly reduced in Cohorts B, C, and D, relative to Cohort A. Hence, both the *mSuv3*+/− nuclear genotype and the *mSuv3*+/− female transmitted mtDNA contributed to the reduction in the mtDNA copy number. Hence, both the nuclear *mSuv3* mutation and the maternally inherited defective mitochondria did contribute to the overall reduction in the mtDNA copy number in the mice.

Since these mitochondrial DNA aberrations may reduce mitochondrial activities, we then examined the biochemical activities of mitochondrial OXPHOS complexes I, II+III and IV, each containing one or more mtDNA encoded subunits. Mitochondria isolated from the

brains of 10-month-old animals in Cohorts B, C, and D showed significantly reduced OXPHOS complex activities than those of Cohort A (Fig. 5C). Therefore, the increased mtDNA mutation rate and reduced mtDNA copy number indeed deteriorate mitochondrial energy production.

To further validate the contribution of mitochondrial aberration to the aforementioned phenotypes observed in *mSuv3*+/− mice, we crossed *mSuv3*+/− with C57/BL6 for two additional generations to obtain sufficient progenies for each cohort. Consistent with our earlier observation, the average lifespan of the third generation of Cohorts C (489 days) and D (534 days) were significantly shorter than that of Cohorts A (732 days) and B (688 days) ($P<0.0001$) (Fig. 5D). Similar to the observation shown in Fig. 3C, we found that Cohorts B, C, and D had tumor incidences approaching 100%, which were significantly higher than the 50% tumor incidence seen in Cohort A. These data further indicated that the reduced lifespan and increased tumor incidence correlate with the mtDNA aberration, rather than the *mSuv3* nDNA genotype, supporting the hypothesis that the defective mtDNA is a key factor to the observed phenotypes.

Mouse embryonic fibroblasts (MEFs) derived from mice with aberrant mtDNA exibit impaired proliferation capability

To determine if this mitochondrial dysfunction would impede cellular function, we generated MEFs from the four cohorts (genotyping shown in Fig. 6A) and measured their proliferation capacity following the 3T3 protocol (16). By this protocol, the Cohort A MEF cells doubled in number every three days for eight passages, after which the cells were arrested in crisis state and the three-day cell counts were comparable to the inoculation levels. In contrast, the cells from Cohorts B, C, and D did not have an initial proliferative phase, but immediately showed low proliferation potential (Fig. 6B), suggesting these fibroblasts might already enter senescence when initially explanted. To determine if the reduced proliferative capacity of the Cohorts B, C, and D could be correlated to the loss of mtDNA integrity, we assessed the mtDNA copy numbers of the four cell cohorts at passage four. The mtDNA copy numbers of the MEFs from Cohorts B, C, and D were apparently less than half of that of Cohort A (Fig. 6C). Collectively, our data suggested that the *mSuv3*+/− nDNA mutation and the maternally transmitted mtDNAs abnormalities leads to impaired MEF proliferation reminiscent of premature cellular senescence.

Breast tumor cells express low amounts of SUV3 compared to nonmalignant cells

As mentioned above, SUV3 is a highly conserved protein during evolution. Given the substantial stimulation in tumor incidence after inactivation of only one allele of *mSuv3* in mice, it is likely that deficiency of SUV3 may also play a similar role in human tumorigenesis. To validate this, we compared the expression of Suv3 mRNA within a cohort of eighteen pairs of breast tumor and adjacent normal tissues. As shown in Fig. 7A, eleven tumor specimens contained significantly reduced Suv3 mRNA. In another cohort with 19 normal tissues and 45 breast tumor specimens, the expression of Suv3 mRNA in tumors was also significantly lower than in normal tissues (Fig. 7B). These data provided us the first clinical evidence to support the notion that reduction of SUV3 expression may participate in human tumorigenesis, which can be resulted from the loss of mtDNA integrity.

Discussion

In this communication, we demonstrated that inactivating one allele of *mSuv3* in mice shortens the lifespan and predisposes the animals to tumor formation with 90% penetrance. Heterozygote offsprings derived from crossing *mSuv3*+/− male with C57/BL6 female live as long as wild type mice whereas those from cronssing *mSuv3*+/− female to C57/BL6 male exhibit shortened lifespan. Moreover, shortened lifespan, reduced fecundity, and multiple tumor formations are seen in *mSuv3*+/+ mice with mitochondria derived from *mSuv3*+/− mother, suggesting the disease phenotypes follow patterns of maternal mitochondrial inheritance. Findings such as higher mutation rates and reduced mtDNA copy numbers are observed in the offsprings with mitochondria derived from *mSuv3*+/− mother, suggesting that SUV3 is a novel tumor suppressor that functions through maintainance of the mitochondrial genome integrity.

Genomic instability is a hallmark of human cancer. Many of the tumor suppressor genes identified so far are critical for maintaining genome stability. For example, the prototypic *RB* gene has been shown to be essential in monitoring chromosome segregation fidelity and cell cycle entrance (17). *p53*, and *BRCA1/2*, participate in maintaining genome stability by regulating DNA damage repair response pathways in additional to other functions (18, 19). For this group of tumor suppressor genes, both alleles are inactivated in tumor cells, but reintroduction of one wild type allele can suppress tumor growth by inducing cell cycle arrest or tumor cell apoptosis (20). On the other hand, another group of tumor susceptibility genes, such as Mismatch repair genes (*MMR*), Werner syndrome gene (*WNS*) and Bloom's syndrome gene (*BLM*), directly participate in DNA repair (21, 22). Defects in *MMR* genes can lead to mutations in the type II TGF-beta receptor, causing Hereditary Non-polyposis Colorectal Cancer (HNPCC) (23). However, different from the previous group of tumor suppressor genes like RB, reintroducing *MMR* gene back to HNPCC cells cannot suppress the tumor progression. The other two genes in this group, *WNS* and *BLM*, both encode RecQ helicases, and inactivating both copies of the genes results in premature ageing and cancer (22). Interestingly, inactivation of one allele of SUV3 helicase in our mouse model appears to trigger an increase of mtDNA mutations and a reduction in the mtDNA copy numbers, an analogy of mitochondrial genomic instability, leading to increased tumor incidences. These mutated and dysfunctional mitochondria are sufficient to enhance tumor formation even when both copies of wild type *mSuv3* were present. The *mSuv3* knockout mice described here provides a unique genetic model to study mitochondrial genomic instability in cancer predisposition.

It is noted that the protein level of SUV3 in mouse is critical for maintaining mitochondria genomic stability since the expression from just one copy of wild type allele is insufficient (Fig. 1). This haploinsufficiency principle appears to be the common mechanism seen in many other transgenic mouse tumor models that inactivating both copies of critical genes, such as *AML1* (24), *p27KIP1* (25), *Lkb1* (26), *CtIP* (27), *Smad4* (28), and *RINT1* (29), usually leads to cell death and embryonic lethality, while inactivation of one allele prediposes the animal to tumorigenesis. More intriguingly, tumor cells derived from these animals frequently keep the remaining wild type allele, instead of losing it as in the case of *RB* or *p53*. If such principle also applies to human cancer, reduction of mtDNA as well as

SUV3 protein should be observed in at least some human cancers. Indeed, when we surveyed two cohorts of human breast tumor specimens, the expression of SUV3 mRNA in tumors is also significantly lower than in normal tissues. These results implicate that a reduction of SUV3 expression may be involved in the tumorigenesis in a portion of human cancers. Thus, any genetic or epigenetic event that reduces the expression of SUV3 may contribute to mitochondria genomic instability and promote tumor formation.

How does inactivating one allele of *mSuv3* lead to mitochondrial genomic instability? SUV3 is known as a component of the mitochondrial RNA degradosome for decades (10, 12, 13). In yeast, we and others have demonstrated that inactivation of the *ySuv3* gene leads to respiratory deficiency and compromised mtDNA integrity (12, 30). In mammalian system, we also observed an accumulation of truncated mitochondrial RNA transcripts and reduction in mtDNA copy number in SUV3 knockdown cells (14). In fact, in addition to its role in RNA degradation (31), mammalian SUV3 has been shown to participate in several DNA processes, including unwinding double stranded DNA substrates (32), and associating with purified mitochondrial nucleoids (33). These potential biochemical activities of SUV3 suggest that SUV3 may be involved in preventing mtDNA mutagenesis and/or facilitating replication. Consistant with this notion, we have demonstrated that SUV3 is associated with actively replicating mitochondrial nucleoids in yeast (30), although a direct biochemical link remains to be demonstrated. Recently, an increase of mtDNA mutations has been observed in mice carrying a mutant POLG, a mtDNA mutator (34, 35, 36). However, the mtDNA copy numbers stayed at the same level as wild type animals (37), suggesting a potentially different mechanism from the role of SUV3 in maintaining mitochondrial genomic stability. It is noted that a small amount of SUV3 localizes to nucleus, where it interacts with BLM helicase (15). However, the precise function of such interaction remains to be established. Although we cannot completely rule out the potential nuclear role of SUV3 impacting on these phenotypes, our backcrossing data (Fig. 3) clearly indicated the maternal effect of SUV3. Regardless the mechanism, mitochondrial dysfunctions resulted from SUV3 insufficiency clearly enhances tumorigenesis, strongly supporting the notion that mitochondrial integrity is important during development and progression of cancers (2, 38). It has been reported that mtDNA mutations are prevalent in colon cancer (39, 40). Therefore, loss of mtDNA integrity may be a general feature for cancer, as the accumulation of mtDNA mutations may increase mitochondrial ROS production, which is a potent mitogen (41, 42). SUV3 as a tumor suppressor operating on mitochondria is conforming with the growing data that both tumor suppressors and oncogenes can target to mitochondrial functions. For example, SIRT3, a newly identified tumor suppressor, is nuclear-encoded but localized to mitochondria (43). In addition, deregulation of metabolic enzymes such as $NADP^+$-dependent isocitrate dehydrogenase enzymes (*IDH1* and *IDH2*) have been linked to human glioma (44, 45). Thus, this new paradigm offers a potential mechanism for a group of human cancers with maternal inheritance otherwise recognized as sporadic cancer.

Experimental procedures and Materials

Construction of *mSuv3* targeting vector

The *Mus musculus Suv3* (*mSuv3*) gene was isolated by screening a mouse 129/Sv genomic library (kindly provided by Dr. Tom Doetschman, University of Cincinnati) using a 2.4-kb fragment of human *SUV3* cDNA as the probe. A 5-kb *BglII* fragment of the mouse *mSuv3* gene was subcloned into the pBluescript SK vector (Stratagene, CA), yielding a pBg5 plasmid. The internal *HindIII* site, corresponding to amino acid residue 684 of human SUV3, was restricted and converted to *SalI* by ligation with a *SalI* linker. A *pgkneopA* cassette (46) in antisense orientation was inserted into the engineered *SalI* site and the resulting plasmid was designated as p*mSuv3*-neo. The *BglII* fragment of *mSuv3*-neo was then subcloned into a p2TK vector (47) to produce the final targeting vector designated as *mSuv3*-KO.

Selection of ES clones

SalI-linearized *mSuv3*-KO targeting vector was electroporated into an E14.1 ES cells and selected in medium containing G418 (250μg/ml) and 2'-fluoro-2'-deoxy-1-β-D-arabinofuranosyl-5-iodo-uracil (FIAU) (1μM). DNA extracted from the resistant ES cell clones was digested with *BamHI-SalI*, and analyzed by Southern blotting. A 0.8-kb *BamHI-BglII* fragment, designated as probe A, corresponding to a region at 5' end of the genomic sequence in the targeting vector, was used to identify bands of 10-kb and 11.6-kb, that correspond to germ line wild type *mSuv3* and the homologous recombinant allele, respectively. An additional DNA probe corresponding to a fragment in the neo gene was also used to identify the neo-containing restriction fragment.

Embryo collection, PCR genotyping, and histology of embryos from *mSuv3* heterozygotes intercrosses

Mice heterozygous (F1) for the *mSuv3* mutant allele were mated and toes from F2 progeny were cut for genotype analysis. Embryos from timed pregnancies were dissected from maternal decidua. For embryos older than E9.5, the visceral yolk sac was collected and genotyped by PCR (48). For E4.5 to E8.5 embryos, uterine embryos were excised and fixed in 4% paraformaldehyde. After embedded in paraffin, the embryos were sectioned and stained with Mayer's hematoxylin and eosin (H&E). Genotypings were performed on the microdissected cells from stained slides. E3.5 blastocysts were flushed from maternal uterus and genotyped by PCR. The targeted allele, a 236 bp product within the *pgkneopA* cassette, was assayed using primers: forward: 5'-TGA TAT TGC TGA AGA GCT TGG CGG C-3'; reverse: 5'-TGG GAG TGG CAC CTT CCA GGG TCA A-3'. The wild type allele, 149 bp product within the targeted exon of the mouse *mSuv3* gene, was assessed using the primers: forward: 5'-TCC AAG AAG GCG TGC ACA ACA TCA C-3'; reverse: 5'-ACT TTT GGT GCC ACG TGT CCT TCT C-3'.

Breeding of *mSuv3* heterozygous mice

The F1 heterozygous *mSuv3*+/− mice were derived from crossing two chimeric mice with C57/BL6 mice, generating a hybrid between the 129SvJ and C57/BL6 inbred backgrounds.

The F1 *mSuv3*+/− mice were then interbred to generate mice with two *mSuv3* genotypes (*mSuv3*+/+ and *mSuv3*+/−). The F2 *mSuv3*+/− mice were interbred to generate F3 *mSuv3* +/+ and *mSuv3*+/− mice. Similarly, F3 *mSuv3*+/− mice were interbred to generate F4 *mSuv3* +/+ and *mSuv3*+/− mice. Since the female F3 and F4 *mSuv3*+/− mice were not very fertile, the *mSuv3* knockout allele was maintained by crossing male F4 *mSuv3*+/− mice to C57/BL6 females. The F1 to F4 mice, which were on a mixed C57/BL6 and 129SvJ backgrounds, were analyzed (Figure 2).

Breeding of *mSuv3* heterozygous Mice into C57/BL6 predominant background

The F3 heterozygous *mSuv3*+/− mice were crossed to C57BL/6 wild type mice, and the progeny were analyzed (Figure 3B). Subsequent crosses for two additional generations were analyzed in Figure 5D.

Fecundity Determination

Female *mSuv3*+/− or *mSuv3*+/+ mice were housed together with C57/BL6 male starting at eight weeks of age. The birth date and number of pups of each delivery were recorded. Pups were weaned at 21 days.

Histology and Immunohistochemistry

Tissues were fixed in 4% paraformaldehyde, paraffin embedded, and stained with H&E. Immunostaining was performed using homemade SUV3 specific mouse monoclonal antibody 18C5 and Vectastain Elite ABC kit (Vector Laboratories, CA).

mtDNA Sequence analysis

Genomic DNA including mtDNA was isolated from aged *mSuv3*+/− mice by the Puregene DNA purification kit (Gentra System Inc, MN). The region surrounding the L-strand origin of DNA replication (O_L fragment nt 4418–6409) was PCR-amplified using PfuUltra DNA polymerase (Agilent, CA) and primers: O_L forward: 5’-TTT CAT AGG GGC ATG AGG AG-3’; O_L reverse: 5’-AAG CAC GAT GTC AAG GGA TG-3’. The PCR products were subcloned into the Zero Blunt PCR cloning vectors (Invitrogen, CA). Forty-eight bacterial clones were isolated for plasmid DNA extraction. Sequencing were performed using primers: 4418F: 5’-TTT CAT AGG GGC ATG AGG AG-3’; 4698F: 5’-ACC ACT AAC AGG ATT CTT ACC-3’; 5262F: 5’-TAT CAC CTT AAG ACC TCT GG-3’; and 5865F:5’-CCC AGC CAT AAC ACA GTA TC-3’.

mtDNA copy number determination

The ratio of mtDNA to nDNA was determined by quantitative real time PCR using the cycling parameters: 95 °C for 5 min, 95 °C for 30s, 58 °C for 45s, for 40 cycles (49, 50). Primer sequences included: mitochondrial 12S rDNA: 12S forward: 5’-ACC GCG GTC ATA CGA TTA AC-3’; 12S reverse: 5’-CCC AGT TTG GGT CTT AGC TG-3’; nuclear 18S rDNA: 18S forward: 5’-CGC GGT TCT ATT TTG TTG GT-3’; 18S reverse: 5’-AGT CGG CAT CGT TTA TGG TC-3’ Determinations of samples and standards were performed in triplicate. The 12S/18S ratios were calculated from the means.

Mitochondrial enzymatic assays

OXPHOS enzyme analysis (51) was performed on isolated mitochondria, which were lyzed by three cycles of freeze-and-thaw in liquid N_2 and 37°C water bath, respectively. OXPHOS complexes I, II+III and IV were assayed immediately using spectrophotometric assays. Complex I activity was measured as the rotenone-sensitive NADH oxidation rate at 340 nm. Complex II+III activity was measured as the cytochrome c (cyt c) reduction rate at 550 nm and complex IV activity as the reduced cytochrome c oxidation rate at 550 nm. Citrate synthase activity was used as a standard to normalize for mitochondria amount.

Isolation and culturing of mouse embryonic fibroblasts (MEFs)

Primary MEF cultures were isolated from individual E12.5 embryos obtained from crossing heterozygous male and female *mSuv3*+/− mice with C57/BL6 mice. The MEFs were expanded for one passage and genotyped by PCR analysis. Complete DMEM with high glucose containing 10% fetal bovine serum, 25 μM/ml sodium pyruvate, 100 units/ml penicillin, and 100 μg of streptomycin was used for culturing MEF cells. For the prolifereation asssays, the MEFs were propagated according to the 3T3 protocol (16), in which the cells were harvested, counted, and 3×10^5 cells were seeded into a new 60-mm dish every three days,. Cell lines were propagated until all MEF cultures entered crisis.

Western blot analysis

Proteins were separated by SDS-PAGE, blotted to Immobilon-P membranes (Milipore, MA) and probed with antibodies against p48 (GeneTex, CA) or SUV3, using a mouse anti-human SUV3 polyclonal antibody generated against the GST-SUV3 fusion protein (amino acids 1–122).

Quantitative real-time PCR assay

Quantitative real-time PCR was performed using Fast SYBR-Green master mix according to the manufacturer's instruction and analyzed on a StepOnePlus Real-Time PCR system (Applied Biosystems, CA). Human SUV3 mRNA levels were calculated according to the relative ΔCt method using β actin mRNA as an internal control. Primers used are: human β actin: ACTB forward: 5’-ATC TGG CAC CAC ACC TTC TAC A-3’; ACTB reverse: 5’-TCA CCG GAG TCC ATC ACG AT-3’; human SUV3: SUV3 forward: 5’-ATC AGG GAG CCA GTC ACG AT-3’; SUV3 reverse: 5’-GCT GGG TGG CTC AGT AGC TT-3’.

Statistical analysis

Except for the quantifications of specific immunoblots, mouse tumorigenesis assay and cell growth assay, all data are presented as means±standard deviation. Student's t-test was used to compare control and treatment groups. Asterisk (*) indicates statistic significance with P-value <0.05.

Acknowledgements

We thank Dennis Wang for his critical reading, Dr. Tom Doetschman for providing 129/Sv mouse genomic library, Andrea Nikitin, Suna Cai, and Weiwei Fan for their excellent assistance. This study was supported by grant NIH AG027877 to WHL and PLC, and NS21328 and AG13154 to DCW. Based on the UCI’s policy, it is declared that

WHL serves as a member of Board of Directors of GeneTex, Inc. This arrangement has been reviewed and approved by UCI COI committee.

Reference

1. Harman D. The biologic clock: the mitochondria? J Am Geriatr Soc. 1972; 20:145–147. [PubMed: 5016631]
2. Wallace DC, Fan W. The pathophysiology of mitochondrial disease as modeled in the mouse. Genes Dev. 2009; 23:1714–1736. [PubMed: 19651984]
3. Attardi G, Schatz G. Biogenesis of mitochondria. Annu Rev Cell Biol. 1988; 4:289–333. [PubMed: 2461720]
4. Golden TR, Melov S. Mitochondrial DNA mutations, oxidative stress, and aging. Mech. Ageing Dev. 2001; 122:1577–1589. [PubMed: 11511398]
5. de Grey AD. The reductive hotspot hypothesis of mammalian aging: membrane metabolism magnifies mutant mitochondrial mischief. Eur J Biochem. 2002; 269:2003–2009. [PubMed: 11985576]
6. Yui R, Ohno Y, Matsuura ET. Accumulation of deleted mitochondrial DNA in aging Drosophila melanogaster. Genes Genet Syst. 2003; 78:245–251. [PubMed: 12893966]
7. Warburg O, Wind F, Negelein E. The metabolism of tumors in the body. J Gen Physiol. 1927; 8:519–530. [PubMed: 19872213]
8. Chatterjee A, Mambo E, Sidransky D. Mitochondrial DNA mutations in human cancer. Oncogene. 2006; 25:4663–4674. [PubMed: 16892080]
9. Golik P, Szczepanek T, Bartnik E, Stepien PP, Lazowska J. The *S. cerevisiae* nuclear gene SUV3 encoding a putative RNA helicase is necessary for the stability of mitochondrial transcripts containing multiple introns. Curr Genet. 1995; 28:217–224. [PubMed: 8529267]
10. Margossian SP, Li H, Zassenhaus HP, Butow RA. The DExH box protein Suv3p is a component of a yeast mitochondrial 3'-to-5' exoribonuclease that suppresses group I intron toxicity. Cell. 1996; 84:199–209. [PubMed: 8565066]
11. Dziembowski A, Piwowarski J, Hoser R, Minczuk M, Dmochowska A, Siep M, et al. The yeast mitochondrial degradosome. Its composition, interplay between RNA helicase and RNase activities and the role in mitochondrial RNA metabolism. J Biol Chem. 2003; 278:1603–1611. [PubMed: 12426313]
12. Stepien PP, Margossian SP, Landsman D, Butow RA. The yeast nuclear gene suv3 affecting mitochondrial post-transcriptional processes encodes a putative ATP-dependent RNA helicase. Proc Natl Acad Sci U S A. 1992; 89:6813–6817. [PubMed: 1379722]
13. Stepien PP, Kokot L, Leski T, Bartnik E. The suv3 nuclear gene product is required for the in vivo processing of the yeast mitochondrial 21s rRNA transcripts containing the r1 intron. Curr Genet. 1995; 27:234–238. [PubMed: 7736607]
14. Khidr L, Wu G, Davila A, Procaccio V, Wallace D, Lee WH. Role of SUV3 helicase in maintaining mitochondrial homeostasis in human cells. J Biol Chem. 2008; 283:27064–27073. [PubMed: 18678873]
15. Pereira M, Mason P, Szczesny RJ, Maddukuri L, Dziwura S, Jedrzejczak R, et al. Interaction of human SUV3 RNA/DNA helicase with BLM helicase; loss of the SUV3 gene results in mouse embryonic lethality. Mech Ageing Dev. 2007; 128:609–617. [PubMed: 17961633]
16. Todaro GJ, Green H. Quantitative studies of the growth of mouse embryo cells in culture and their development into established lines. J Cell Biol. 1963; 17:299–313. [PubMed: 13985244]
17. Zheng L, Lee WH. Retinoblastoma tumor suppressor and genome stability. Adv Cancer Res. 2002; 85:13–50. [PubMed: 12374284]
18. Chen PL, Chen Y, Bookstein R, Lee WH. Genetic mechanisms of tumor suppression by the human p53 gene. Science. 1990; 250:1576–1580. [PubMed: 2274789]
19. Ting NS, Lee WH. The DNA double-strand break response pathway: becoming more BRCAish than ever. DNA Repair (Amst). 2004; 3:935–944. [PubMed: 15279779]
20. Riley DJ, Lee EY, Lee WH. The retinoblastoma protein: more than a tumor suppressor. Annu Rev Cell Biol. 1994; 10:1–29. [PubMed: 7888173]

21. Rowley PT. Inherited susceptibility to colorectal cancer. Annu Rev Med. 2005; 56:539–554. (2005). [PubMed: 15660526]
22. Hickson ID. RecQ helicases: caretakers of the genome. Nat Rev Cancer. 2003; 3:169–178. [PubMed: 12612652]
23. Markowitz SD, Wang JY, Myeroff L, Parsons R, Sun L, Lutterbaugh J, et al. Inactivation of the type II TGF-beta receptor in colon cancer cells with microsatellite instability. Science. 1995; 268:1336–1338. [PubMed: 7761852]
24. Okuda T, van Deursen J, Hiebert SW, Grosveld G, Downing JR. AML1, the target of multiple chromosomal translocations in human leukemia, is essential for normal fetal liver hematopoiesis. Cell. 1996; 84:321–330. [PubMed: 8565077]
25. Fero ML, Randel E, Gurley KE, Roberts JM, Kemp CJ. The murine gene p27Kip1 is haplo-insufficient for tumour suppression. Nature. 1998; 396:177–180. [PubMed: 9823898]
26. Bardeesy N, Sinha M, Hezel AF, Signoretti S, Hathaway NA, Sharpless NE, et al. Loss of the Lkb1 tumour suppressor provokes intestinal polyposis but resistance to transformation. Nature. 2002; 419:162–167. [PubMed: 12226664]
27. Chen PL, Liu F, Cai S, Lin X, Li A, Chen Y, et al. Inactivation of CtIP leads to early embryonic lethality mediated by G1 restraint and to tumorigenesis by haploid insufficiency. Mol Cell Biol. 2005; 25:3535–3542. [PubMed: 15831459]
28. Alberici P, Jagmohan-Changur S, De Pater E, Van Der Valk M, Smits R, Hohenstein P, et al. Smad4 haploinsufficiency in mouse models for intestinal cancer. Oncogene. 2006; 25:1841–1851. [PubMed: 16288217]
29. Lin X, Liu CC, Gao Q, Zhang X, Wu G, Lee WH. RINT-1 serves as a tumor suppressor and maintains Golgi dynamics and centrosome integrity for cell survival. Mol Cell Biol. 2007; 27:4905–4916. [PubMed: 17470549]
30. Guo XE, Chen CF, Wang DD, Modrek AS, Phan VH, Lee WH, et al. Uncoupling the Roles of the SUV3 Helicase in Maintenance of Mitochondrial Genome Stability and RNA Degradation. J Biol Chem. 2011; 286:38783–38794. [PubMed: 21911497]
31. Wang DD, Shu Z, Lieser SA, Chen PL, Lee WH. Human mitochondrial SUV3 and polynucleotide phosphorylase form a 330-kDa heteropentamer to cooperatively degrade double-stranded RNA with a 3'-to-5' directionality. J Biol Chem. 2009; 284:20812–20821. [PubMed: 19509288]
32. Shu Z, Vijayakumar S, Chen CF, Chen PL, Lee WH. Purified human SUV3p exhibits multiple-substrate unwinding activity upon conformational change. Biochemistry. 2004; 43:4781–4790. [PubMed: 15096047]
33. Bogenhagen DF, Rousseau D, Burke S. The layered structure of human mitochondrial DNA nucleoids. J Biol Chem. 2008; 283:3665–3675. [PubMed: 18063578]
34. Trifunovic A, Wredenberg A, Falkenberg M, Spelbrink JN, Rovio AT, Bruder CE, et al. Premature ageing in mice expressing defective mitochondrial DNA polymerase. Nature. 2004; 429:417–423. [PubMed: 15164064]
35. Kujoth GC, Hiona A, Pugh TD, Someya S, Panzer K, Wohlgemuth SE, et al. Mitochondrial DNA Mutations, Oxidative Stress, and Apoptosis in Mammalian Aging. Science. 2005; 309:481–484. [PubMed: 16020738]
36. Vermulst M, Bielas JH, Kujoth GC, Ladiges WC, Rabinovitch PS, Prolla TA, et al. Mitochondrial point mutations do not limit the natural lifespan of mice. Nature Genet. 2007; 39:540–543. [PubMed: 17334366]
37. Trifunovic A, Hansson A, Wredenberg A, Rovio AT, Dufour E, Khvorostov I, et al. Somatic mtDNA mutations cause aging phenotypes without affecting reactive oxygen species production. Proc Natl Acad Sci U S A. 2005; 102:17993–17998. [PubMed: 16332961]
38. Zanssen S, Schon EA. Mitochondrial DNA Mutations in Cancer. PLoS Med. 2005; 2:e401. [PubMed: 16288567]
39. Polyak K, Li Y, Zhu H, Lengauer C, Willson JK, Markowitz SD, et al. Somatic mutations of the mitochondrial genome in human colorectal tumours. Nature Genet. 1998; 20:291–293. [PubMed: 9806551]

40. He Y, Wu J, Dressman DC, Iacobuzio-Donahue C, Markowitz SD, Velculescu VE, et al. Heteroplasmic mitochondrial DNA mutations in normal and tumour cells. Nature. 2010; 464:610–614. [PubMed: 20200521]
41. Burdon RH. Superoxide and hydrogen peroxide in relation to mammalian cell proliferation. Free Rad Biol Med. 1995; 18:775–794. [PubMed: 7750801]
42. Wallace DC, Fan W, Procaccio V. Mitochondrial energetics and therapeutics. Annu Rev Pathol. 2010; 5:297–348. [PubMed: 20078222]
43. Kim HS, Patel K, Muldoon-Jacobs K, Bisht KS, Aykin-Burns N, Pennington JD, et al. SIRT3 is a mitochondria-localized tumor suppressor required for maintenance of mitochondrial integrity and metabolism during stress. Cancer Cell. 2010; 17:41–52. [PubMed: 20129246]
44. Yan H, Parsons DW, Jin G, McLendon R, Rasheed BA, Yuan W, et al. IDH1 and IDH2 mutations in gliomas. N Engl J Med. 2009; 360:765–773. [PubMed: 19228619]
45. Xu W, Yang H, Liu Y, Yang Y, Wang P, Kim SH, et al. Oncometabolite 2-hydroxyglutarate is a competitive inhibitor of Éø-ketoglutarate-dependent dioxygenases. Cancer Cell. 2011; 18:17–30. [PubMed: 21251613]
46. Soriano P, Montgomery C, Geske R, Bradley A. Targeted disruption of the c-src proto-oncogene leads to osteopetrosis in mice. Cell. 1991; 64:693–702. [PubMed: 1997203]
47. Lee EY-HP, Chang C-Y, Hu N, Wang Y-CJ, Lai C-C, Herrup K, et al. Mice deficient for Rb are nonviable and show defects in neurogenesis and haematopoiesis. Nature. 1992; 359:288–294. [PubMed: 1406932]
48. Liu CY, Flesken-Nikitin A, Li S, Zeng Y, Lee W-H. Inactivation of the mouse Brca1 gene leads to failure in the morphogenesis of the egg cylinder in early postimplantation development. Genes Dev. 1996; 10:1835–1843. [PubMed: 8698242]
49. Rodríguez-Santiago B, Casademont J, Nunes V. Is mitochondrial DNA depletion involved in Alzheimer's disease? Eur J Hum Genet. 2001; 9:279–285. [PubMed: 11313772]
50. Coskun PE, Beal MF, Wallace DC. Alzheimer's brains harbor somatic mtDNA control-region mutations that suppress mitochondrial transcription and replication. Proc Natl Acad Sci U S A. 2004; 101:10726–10731. [PubMed: 15247418]
51. Trounce IA, Kim YL, Jun AS, Wallace DC. Assessment of mitochondrial oxidative phosphorylation in patient muscle biopsies, lymphoblasts, and transmitochondrial cell lines. Methods Enzymol. 1996; 264:484–509. [PubMed: 8965721]

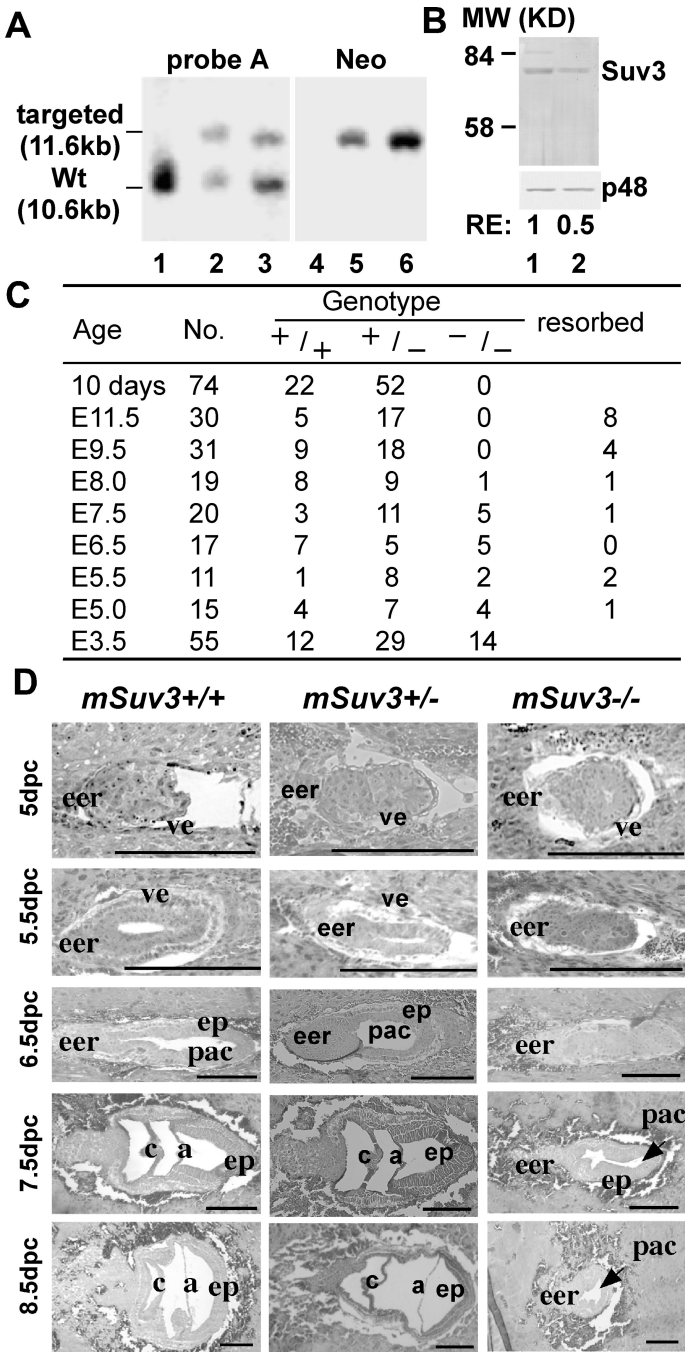

C

Age	No.	Genotype +/+	Genotype +/−	Genotype −/−	resorbed
10 days	74	22	52	0	
E11.5	30	5	17	0	8
E9.5	31	9	18	0	4
E8.0	19	8	9	1	1
E7.5	20	3	11	5	1
E6.5	17	7	5	5	0
E5.5	11	1	8	2	2
E5.0	15	4	7	4	1
E3.5	55	12	29	14	

Figure 1.

Targeted disruption of the mouse *mSuv3* locus leads to embryonic lethality. (A) Confirmation of the targeted disruption of the *mSuv3* allele. DNA samples from parental El4.1 cells (lanes 1 & 4) and two candidate recombinant clones [mSuv3-ko 5 (lanes 2 & 5) and mSuv3 ko 149 (lanes 3 & 6)] were digested with *SalI-BamHI* and probed with either probe A or the *neo* probe. An additional fragment of the expected size of 11.6 kb was found in each of the recombinant clones. (B) Western blot analysis of SUV3 protein level. Whole-cell lysate of MEFs of wild type (lane 1) and heterozygote (lane 2) were separated by SDS-

PAGE and probed with an antibody against SUV3. p48 was used as a loading control. (C) Genotypes of offspring from heterozygous mSuv3+/− mice intercross. Pregnant females of mSuv3+/− intercrosses were sacrificed and the fetuses examined at different gestation times from E3.5 to E11.5 days. (D) Developmental abnormalities of *mSuv3* mutant embryos. Histological analysis was performed on embryo sections of wild type and *mSuv3*−/− conceptuses. The uteri of *mSuv3*+/− females were dissected between 5.0 and 8.0 days after intercross, and 4 μm sections were prepared. All uterine decidua were sectioned transversely and labeled as described (48). The mesometrial to anti-mesometrial axis is from left to right. Abbreviations: (eer) extraembryonic region; (ve) viceral endoderm; (ep) epiblast; (pac) proamniotic cavity; (c) chorion; (a) amnion. Bar, 100 μm.

A

Generation	F1	F2	F3	F4
Lifespan (days)	801.3 ±26.4	718.6 ±20.4	622.4 ±36.7	509.2 ± 37.7
Mice No.	26	30	24	28

F1:F2 P = 0.015,F2:F3 P = 0.019,F3:F4 P = 0.037

B

Tumor type	Generation			
	F1	F2	F3	F4
Lymphoma	14	10	11	15
Papillary adenocarcinoma	3	6	1	3
Lung adenocarcinoma	5	2	1	1
Gastric or small intestine adenoma	1	1	1	1
Pituitary adenoma	1		1	
Sebaceous sarcoma	1			
Bladder transitional cell carcinoma	1	1	1	
Bladder sarcoma		2		
Mammary carcinoma			1	
Mammary papilloma		1		
Hepatocellular carcinoma	1	3		
Squamous cell carcinoma	1	2		
Ovary cystadenoma		1	2	
Total of tumor-bearing mice	21	22	14	19
Total mice number	23	26	17	21
% of tumor-bearing mice	85.7	84.6	82.4	90.5

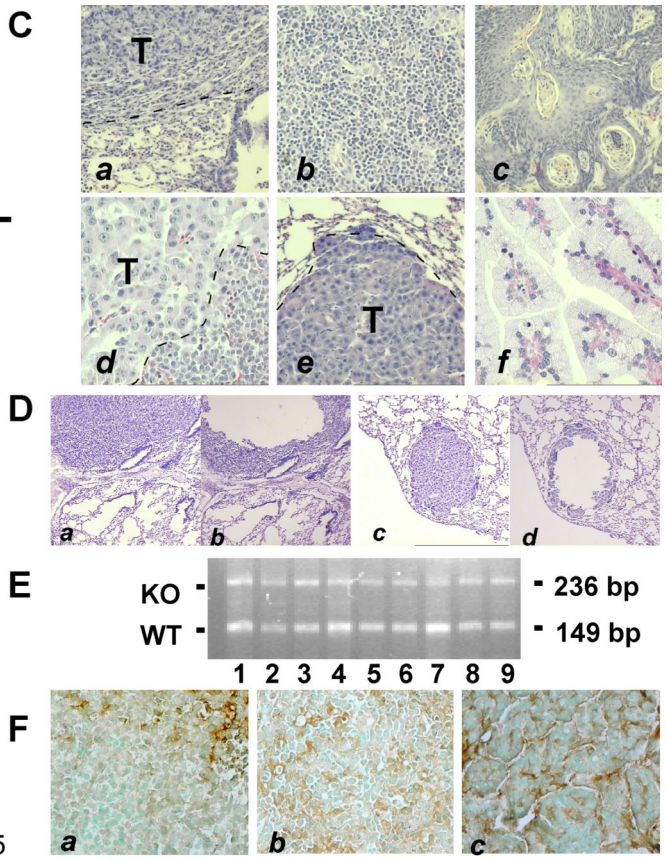

Figure 2.

Lifespan and tumor spectra of the heterozygous offspring derived from *mSuv3*+/− intercross mice. (A) Shortened lifespan of *mSuv3* heterozygotes at different intercross generations. (B) Tumor incidence and spectra of *mSuv3*+/− intercross mice. (C) H&E histology of *mSuv3*+/− mouse tumors: lung adenocarcinoma (a), high-grade lymphoma (b), squamous cell carcinoma (c), pituitary adenoma (d), metastasis – hepatocyte carcinoma (e) and papillary adenocarcinoma (f). (D) Microdissected tumors of *mSuv3*+/− mice. Micrographs showed paraffin-sections of lung adenocarcinoma (a & b) and lung metastatic HCC (c & d) before (a & c) and after (b & d) microdissection. (E) Genotyping of *mSuv3* alleles in the tumor samples (wt: 149 bp: KO: 236 bp) (F) Immunostaining with anti-SUV3 antibodies demonstrated tumors derived from *mSuv3*+/− mice expressing SUV3.

A. Tumorigenicity of *mSuv3+/+; mt-msuv3+/-* offspring of *mSuv3+/-* mice intercross

Tumor type	Tumor No.
Lymphoma	8
Papillary adenocarcinoma	2
Lung adenocarcinoma	1
Gastric adenoma	3
Pituitary adenoma	1
Sebaceous sarcoma	1
Hepatocellular carcinoma	4
Ovary cystadenoma	1
Total of tumor-bearing mice	19
Total mice number	19
% of tumor-bearing mice	100
Average lifespan of mice(days)	485±16

B. mSuv3 +/- mice cross with wildtype C57/BL6

Parent / *mSuv3+/-* offspring	♂Wt X ♀mSuv3+/-	♀ Wt X ♂mSuv3+/-
Lifespan (days)	559± 81	782± 50
Mice number	5	7

(P=0.033)

C. Tumorigenicity of *mSuv3+/+; mt-msuv3+/-* offspring of *mSuv3+/-* female and wildtype C57/BL6 male

Tumor type	Mice No.
Lymphoma	7
Pituitary adenoma	4
Total of tumor-bearing mice	10
Total mice number	10
% of tumor-bearing mice	100
Average lifespan of mice(days)	631± 42

Figure 3.

Mitochondrial function is a dominant determinant for *mSuv3* inheritance. (A) Tumor incidence and spectra of *mSuv3+/+; mt-msuv3+/−* offspring of *mSuv3* heterozygote intercross. (B) Lifespan of heterozygous offsprings derived from either crossing a *mSuv+/−* female to a wild type C57/BL6 male or crossing a wild-type female and a *mSuv+/−* male. (C) Tumor incidence of *mSuv3+/+* offspring from the cross of *mSuv3* heterozygous female and wild type C57/BL6 male (*mSuv3+/+; mt-msuv3+/−*).

A. F1 *mSuv3+/-*

♀ ID	Litter No	Pups/litter	Dead pups
722	3	9, 8, 9	—
724	3	3, 1, 6	—
727	3	6, 8, 8	—
726	4	5, 1, 6, 4	—
729	4	6, 10, 5, 7	—

B. F2 *mSuv3+/-*

♀ ID	Litter No	Pups/litter	Dead pups
317	2	4,1	—
314	3	4, 4, 6	—
212	2	7, 3	—
491	4	5, 8, 1, 3	—
492	4	6, 8, 2, 8	—

C. F3 *mSuv3+/-*

♀ ID	Litter No	Pups/litter	Dead pups
660	1	7	—
16	3	5, 5, 5	0, 2, 1
413	4	5, 7, 2, 7	0, 0, 2, 0
415	4	6, 5, 2, 5	5, 0, 2, 0
418	0	0	—

D. F4 *mSuv3+/+:mt suv3 +/-*

♀ ID	Litter No	Pups/litter	Dead pups
653	1	1	—
652	2	4 , 5	—
624	1	3	3
606	0	0	—
607	0	0	—

Figure 4.

The fecundity is significantly reduced in the third generation of *mSuv3* heterozygous mice. Designated female mice were housed together with C57/BL6 male since 8 weeks old; the number of pups of each delivery and litter were recorded to determine the fecundity of female mice.

A. mtDNA mutation load

	mSuv3 genotype	MtDNA origin	MtDNA Sequenced (kb)	Mutation number	Mutation rate (per 10kb)
A	+/+	+/+	35.7	7	1.96
B	+/-	+/+	36	21	5.8
C	+/+	*mSuv3*+/-	32	17	5.3
D	+/-	*mSuv3*+/-	37.6	21	5.6

B. Relative ratio of mtDNA/nDNA copy number

A	B	C	D
3.55	2.7	2.3	2.7
3.43	2.43	3.8	2.46
4.65	1.74	2.86	1.72
4.99	3.1	1.6	1.33
2.3	2.43	1.66	1.55
4.37	1.82	1.67	0.61
4.8	2.07	2.83	1.85
2.7		3.56	2.35
3.85±1.0	2.32±0.49	2.54±0.86	1.82±0.68

A:B P=0.0003 A:C P=0.0144 A:D P=0.0031

C.

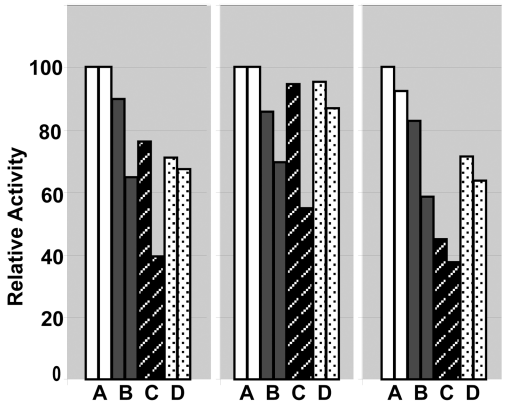

D. Tumor incidence and lifespan of offspring of third generation of cohorts A, B, C, and D

	mSuv3 genotype	MtDNA origin	No. of mice	Mean lifespan	%Tumor-bearing mice
A	+/+	+/+	10	732.0±28.0	50.0%
B	+/-	+/+	15	688.8±36.4	100%
C	+/+	*mSuv3*+/-	19	489.5±18.7	89.4%
D	+/-	*mSuv3*+/-	28	534.7±23.9	92.8%

Lifespan comparison: A:B P=0.399 C:D P=0.180
A:C P<0.0001 A:D P<0.0001
B:C P<0.0001 B:D P=0.0007

Figure 5.

Defective mitochondria inherited from *mSuv3*+/− female leads to increased tumorigenicity and reduced lifespan regardless of nuclear genotype. The offspring from the cross of *mSuv3*+/− female with C57/BL6 male and *mSuv3*+/− male with C57/BL6 female were designated as four cohorts: Cohort A (*mSuv3*+/+; *mt-msuv3*+/+); Cohort B, (*mSuv3*+/−; *mt-msuv3*+/+); Cohort C, (*mSuv3*+/+; *mt-msuv3*+/−); and Cohort D (*mSuv3*+/−; *mt-msuv3*+/−). (A) The region surrounding the mtDNA L-strand origin was sequenced and mtDNA mutation rates were calculated from brain samples collected from ten-month-old mice in

each cohort. (B) The mtDNA to nDNA copy number ratio was determined from seven to eight spleens of 15-month-old mice of each cohort by quantitative real-time PCR using mitochondrial 12S rDNA and nuclear 18S rDNA gene primers (Student's t-test was used to assess P value). (C) Enzyme activities of OXPHOS complexes containing mtDNA encoded subunits, complexes I, II +III, and IV, assessed on brain mitochondria of 10-month-old animals from each cohort. (D) Lifespan and tumor incidence of the offspring (the third generation) derived from *mSuv3*+/− backcross with C57/BL6 mice. (Student's t-test was used to assess P value).

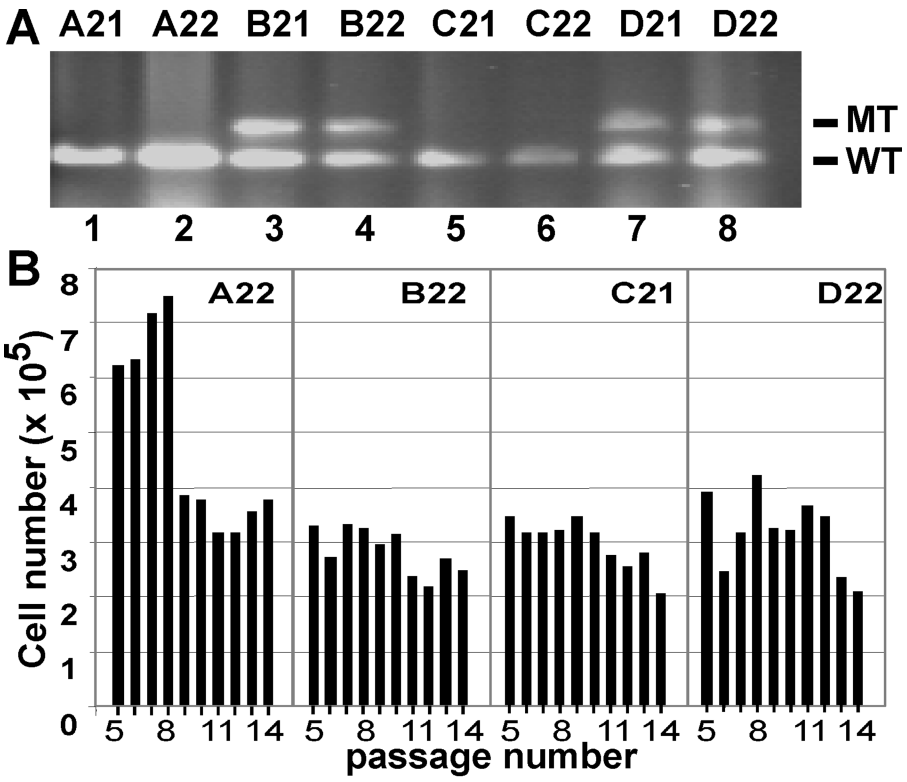

C. Relative ratio of mtDNA/nDNA copy number

A	B	C	D
36.0	6.1	10.7	8.1
29.9	2.4	9.4	9.5
34.8	11.3	10.1	7.2
21.6	9.3	13.8	16.3
20.5	15.8	14.4	13.3
21.2	10.4	8.8	6.9
21.8	10.9	14.3	14.4
20.3	8.9	6.6	10.3
26.9 ± 8.8	9.4 ± 3.9	11.0 ± 2.9	10.3 ± 3.8
A:B P=0.0002		A:C P=0.0003	A:D P=0.0002

Figure 6.

Reduction of mtDNA copy number correlates with reduced MEF cell proliferation. (A) Genotyping of *mSuv3* MEFs. (wt: 149bp, KO: 236bp): Cohort A (*mSuv3*+/+:*mt-msuv3*+/+) = A21 and A22; Cohort B (*mSuv3*+/−: *mt-msuv3*+/+) = B21 and B22; Cohort C (*mSuv3*+/+: *mt-msuv3*+/−) = C21 and C22; and Cohort D (*mSuv3*+/−: *mt-msuv3*+/−) = D21 and D22. (B) Proliferation capacity of MEFs. MEFs prepared from an embryo of each strain were serially passaged following 3T3 protocol. Each plot represents MEFs from a single embryo, with cell numbers on the Y-axis against passage numbers on the X-axis. Each data point was

the mean of two calculations. Standard deviations were too small to be visible. (C) Quantification of relative mtDNA copy number of MEFs from each cohorts at forth passage (mean +/− s.e.m; n=8).

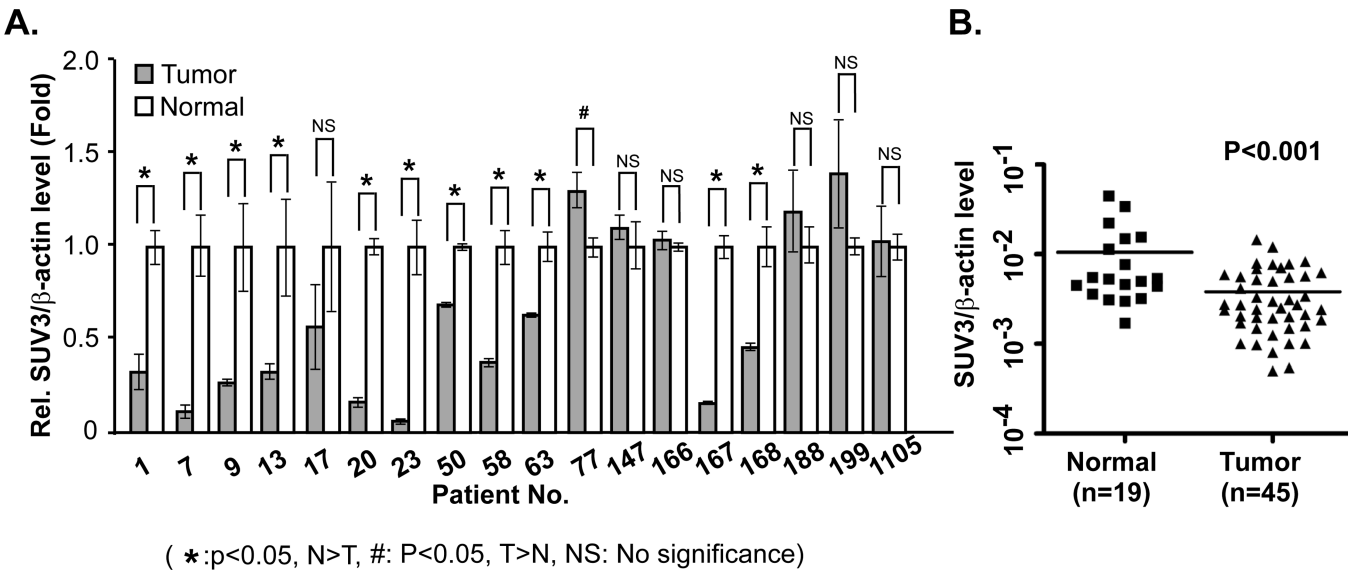

Figure 7.

Reduced SUV3 expression in human tumors. (A) The relative expression level of SUV3 in tumor sample was compared to that of the normal adjacent tissue. Relative expression level of SUV3 gene normalized by β-actin. (B) Comparison of the expression level of SUV3 in normal breast tissue and breast tumor (Student's t-test was used to assess P value).